ACS Sustainable Chemistry & Engineering

Research Article

pubs.acs.org/journal/ascecg

Synthesis and Properties of Alkoxysilane Castor Oil and Their Polyurethane/Urea−Silica Hybrid Coating Films

Shaik Allauddin, Ramanuj Narayan, and K. V. S. N. Raju*

Polymers & Functional Materials Division, Indian Institute of Chemical Technology, Hyderabad-500007, India

ABSTRACT: This paper investigates the structural modifications of castor oil, a renewable resource, to develop functional organic inorganic hybrid coatings. A novel methodology has been developed to introduce hydrolyzable −Si−OCH_3 groups in the castor oil backbone that has been used subsequently for the development of polyurethane/urea−silica hybrid coatings. The alkoxysilane functional castor oil (ASCO) was characterized by techniques such as ^{1}H, ^{13}C, and ^{29}Si nuclear magnetic resonance spectroscopy (NMR), Fourier transform infrared (FTIR) spectroscopy, gel permeation chromatography (GPC), differential scanning calorimetry (DSC), and thermogravimetric analysis (TGA). The ASCO was further reacted with different ratios of isophorone diisocyanate (IPDI) to get an isocyanate-terminated hybrid polyurethane prepolymer that was cured under atmospheric moisture to get the desired coating films. The glass transition temperatures (Tg) of the hybrid networks were found to be in the range of 29−70 °C, and the water contact angles were in the range of 75°−82°. The Tg and hydrophobic character of the hybrid coating films found to increase with an increasing NCO/OH ratio. The thermo-mechanical, viscoelastic, swelling, morphological, and contact angle properties of these films were evaluated. The alkoxy silane-modified castor oil-based coatings have shown better mechanical and viscoelastic properties in comparison to the control (unmodified castor oil) coatings. This work provides an effective and promising way to prepare hydrolyzable silane functional castor oil for high performance hybrid coatings.

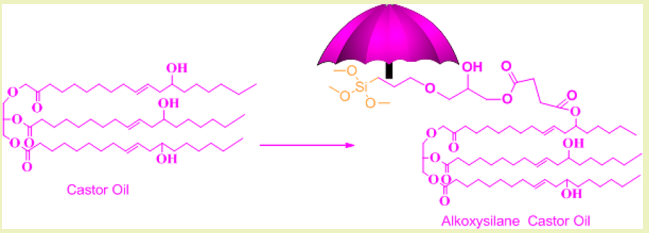

KEYWORDS: *Castor oil, Alkoxy silane, Glass transition, Polyurethanes, Swelling, Thermal*

INTRODUCTION

In recent years, there has been enormous growth on the use of renewable resources to replace petroleum-based polymeric materials for coating development. Natural oils are emerging as an ideal alternative renewable chemical feedstock because oils derived from both plant and animal sources are found in abundance in the world and at relatively lower cost.[1] Castor oil (CO), a renewable resource, is a relatively inexpensive plant oil obtained from the seed of *Ricinus communis*.[2] Additionally, natural hydroxylated castor oil, extracted from castor beans, has played an important role in the formative years of the polyurethane industry before the availability of synthetic polyols. Because of its hydroxy functionality, this oil is suitable for isocyanate reactions to make polyurethane elastomers, adhesives, coatings, interpenetrating polymer networks, etc.[3−6] CO-based polymeric materials are well known for their water resistance and flexibility; however, they do not show properties of rigidity and strength required for structural applications by themselves due to low functionality and relatively lower reactivity due to secondary hydroxyl groups. Organic−inorganic hybrids (OIH), due to their unexpected hybrid properties derived from unique combinations of each component, have drawn considerable interest in recent times.[7] The versatile organofunctional silane coupling agent provides unique opportunities for the development of hybrids containing inorganic filler and organic polymer with improved adhesion and mechanical properties such as tensile strength, impact strength, and abrasion resistance.[8,9] The cross-linking reactions that occur during formation of OIH materials can increase the chemical stability or resistance to swelling of the organic component, and the covalent linkages between the organic and inorganic components improve the homogeneity of the silica network within the organic matrix with excellent film properties and good biodegradability.[10]

There are several routes to prepare hybrid materials, but one of the most widely used methods is the sol−gel technique. One of the attractive features is the generation of an inorganic phase within the organic polymer matrix after moisture cured hydrolyzed silanols undergo condensation with other silanols in the medium, thus leading to cross links.[11] OIH coatings have been developed with plant oils and metal (Ti and Zr) oxides.[12−14] Gallegos et al.[15] have developed hybrid polyurethane for calcified tissue repairing. Galià et al.[16] synthesized silicon-containing polyurethanes with enhanced flame-retardant properties and polyurethane networks with potential applications in biomedicine. Lligadas et al.[17] prepared new class of bionanocomposite materials from linseed oil. Hiroshi et al.[18] developed green nanocomposites with an acid-catalyzed curing of epoxidized plant oils in the presence of organophilic clay. de Luca et al.[19] synthesized novel OIH films through the reaction of epoxidized castor oil with glycidoxypropyltrimethoxysilane and

Received: December 21, 2012
Revised: April 13, 2013
Published: May 9, 2013

Scheme 1. Synthetic Route for Alkoxy Silane Castor Oil

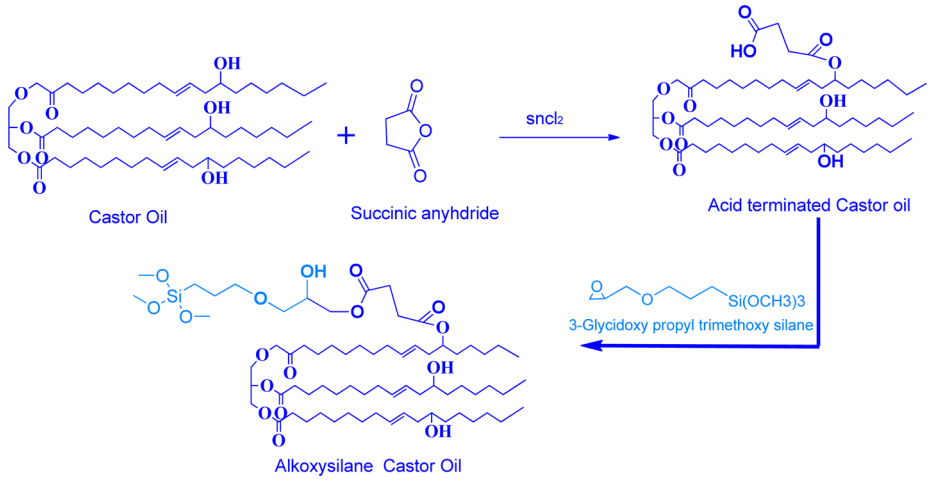

Table 1. Characteristics of CO, COSA, and ASCO

				polydispersity					
sample code	M_w	Mn	Mz	M_w/M_n	Mz/M_w	HV	AV	Tg (°C)	viscosity (η) (mPa s) at 25 °C
CO	1181	1150	1205	1.02	1.02	165	3	−13.1	220
COSA	1442	1235	1668	1.16	1.15	135	26	−15.2	227
ASCO	1512	1302	1754	1.16	1.15	159	2	−14.4	225

tetraethoxysilane. These films have shown good adhesion on aluminum surfaces, and the hardness and tensile strength were found to be increased with increasing amounts of inorganic precursors. Uyama et al.[20] developed oil-based hybrid materials with acid-catalyzed curing of epoxidized triglycerides in the presence of an organophilic montmorillonite (a modified clay), and the hybrids have shown high thermal stability. In all these materials, incorporation of silicones in the polymeric matrix have improved the properties due to many unusual features. Even addition of a very small amount of silicones can cause a crucial improvement in the properties of modified materials. We have also observed a continuously growing interest in applications of reactive silanes and renewable resources in many different fields of materials science and chemical technology.

Most of the hybrid materials have been developed by methods involving addition of external organosilane coupling groups. However, in our attempt to find new applications and uses for CO, we have investigated the synthesis of an alkoxy silane castor oil (ASCO) functional compound through 3-glycidoxypropyl-trimethoxy silane (GPTMS) by chemical reaction. Herein, we describe the synthesis as well as thermal and mechanical properties, contact angle, and morphological and swelling properties of hybrid films based on ASCO (Scheme 1). To develop a high-performance moisture curable coating composition, we studied the effect of the NCO/OH ratio on ASCO and how it affects the thermo-mechanical properties in moisture curable processes. ASCO reacted with IPDI at different NCO/OH equiv ratios to get NCO-terminated hybrid prepolymers. The physical and thermal properties were studied using differential scanning calorimetry (DSC), thermogravimetric analysis (TGA), dynamic mechanical thermal analysis (DMTA), and tensile property measurements. Our research efforts are focused on the development of a novel synthesis method for hybrid composites, which can be a potential candidate for replacing or partially replacing petroleum-based polyurethane hybrids.

EXPERIMENTAL SECTION

Materials. Castor oil was obtained from the local market, with characteristic properties of hydroxyl no. 160−165 mg/KOH g^{-1} and an acid value of 3 mg/KOH g^{-1}. Isophorone diisocyanate (IPDI) and succinic anhydride (SA) were supplied by Alfa Aesar (Ward Hill, MA, U.S.A.). 3-Glycidoxypropyltrimethoxysilane (GPTMS) was supplied by Dynasilan, Germany. Dibutyltin dilaurate (DBTDL) was obtained from Aldrich (Milwaukee, WI, U.S.A.). All other chemicals were analytical grade and were used without further purification.

Synthesis of Acid-Terminated Castor Oil. The CO was dried in a vacuum for 6 h at 70 °C in an oil bath before being used. The dried CO and SA were placed in a three-necked round-bottomed flask equipped with a mechanical stirrer and thermometer. Acid-terminated castor oil (COSA) was synthesized in a four-necked reaction flask by charging CO (20 g) and SA (0.4 g) in a weight ratio. The reaction was maintained at 100 °C in the presence of 1 wt % of $SnCl_2$ as a catalyst. The reaction was stopped when the anhydride peak at 1850 cm^{-1} disappears in the FTIR spectra. The modified oil was named COSA. The acid value (AV) and hydroxyl value (OHV) of COSA were measured according to ASTM standards D 1639-89 and D 4274-94, respectively. Their characteristics are summarized in Table 1. The reaction scheme for the synthesis of the COSA is shown in Scheme 1. ^{1}H NMR ($CDCl_3$, 500 MHz): δ (ppm) = 0.85−0.89 (s, CH_3), 1.22−1.25 (broad singlet, CH_2 chain), 1.31−1.45 (CH═CH−CH_2−CH(OH)−CH2), 2.2 (CH═CH−CH_2−CH-(OH)−CH_2), 5.4−5.5 (d, CH═C H), 5.3(−OH), 4.13 (m, CH-(OCO)CH_2CH_2COOH), 2.55 (CH(OCO)CH_2CH_2COOH), 2.65 (CH(OCO)CH_2CH_2COOH). ^{13}C NMR ($CDCl_3$,125 MHz): δ(ppm) = 72 (CH═CH−CH_2−CH(OH)C H_2),75.1(−CH═CH−CH_2−CH-(OCO)CH_2),174.4(CH(OCO)CH2CH_2COOH),173.1 (CH(OCO)-CH_2 CH_2COOH).

Synthesis of Alkoxy Silane Castor Oil. ASCO was synthesized by charging COSA, GPTMS (0.01 mol), and triethylamine catalyst into a two-necked flask placed over an isomantle bath equipped with mechanical stirrer and nitrogen inlet. The reactant mixture was slowly heated to 75 °C and maintained at 75−80 °C under a nitrogen atmosphere for complete reaction of epoxy groups. The reaction was monitored periodically by FTIR analysis and by determining acid value (AV) of the reaction product. The reaction was stopped when the epoxy peak at 910 cm^{-1} disappeared in FTIR. The modified oil was named

dx.doi.org/10.1021/sc3001756 | ACS Sustainable Chem. Eng. 2013, 1, 910−918

ASCO. The characteristics of the obtained oils are summarized in Table 1. The products were further characterized by FTIR and ^{1}H and ^{13}C NMR. ^{1}H NMR ($CDCl_3$, 500 MHz): δ(ppm) = 4.19(−OCH_2CH-(OH)CH_2O−), 4.14(−$OCH_2CH(OH)CH_2O$−), 3.59 (−OCH_2CH-(OH)CH_2O−), 3.56 (s,Si−OCH_3), 3.55 (−OCH_2 CH (OH)CH_2O−), 3.41 (t,$SiCH_2CH_2CH_2O$), 1.65 (q, $SiCH_2CH_2CH_2O$), 0.65 (t,$SiCH_2CH_2CH_2O$−). ^{13}C NMR ($CDCl_3$,125 MHz):δ(ppm) = 72.8(−$CH_2OCH_2CH(OH)$), 72 (−$CH_2OCH_2CH(OH)$), 70.8 (−$CH_2OCH_2CH(OH)$), 50.5 ($Si(OCH3)_3$), 23.7 (−$SiCH_2CH_2CH_2CH_2$−), 22.55 (−$SiCH_2CH_2CH_2O$−), 9.52 (−$SiCH_2CH_2CH_2CH_2$−), 4.9 ($SiCH_2CH_2CH_2O$−).

Synthesis of Polyurethane/Urea Hybrid Films. The hybrid composites were prepared using the formulation as summarized in Table 2. ASCO was further reacted with IPDI in the presence of 0.01 wt % of DBTL as catalyst with different NCO/OH equiv ratios of 1.2:1, 1.4:1, and 1.6:1 at around 70−80 °C to get different −NCO-terminated hybrid prepolymers. The above-prepared −NCO-terminated hybrid prepolymers (ASCOPU) were used further for the preparation of the final coatings. The hybrid −NCO-terminated prepolymer films were cast on tin foil supported on a glass plate using a manual driven square applicator. The films were kept in an atmospheric moisture and laboratory humidity condition for 40 days for moisture curing and also to carry out the hydrolysis reactions of the alkoxy silane groups of ASCO. Thus, the silanol groups e condensed to form Si−O−Si cross links. They were removed from the glass plate, and the free films of the coatings were obtained by amalgamation technique. The disappearance of −NCO peak at 2270 cm^{-1} from FTIR spectroscopy was taken as a measure of complete cure. The compositions of the different hybrid composites and mole ratios are shown in Table 2.

Table 2. Various Mole Ratios Used To Prepare Different Hybrid Coatings

sample code	IPDI (OH:NCO)
ASCOPU2	1:1.2
ASCOPU4	1:1.4
ASCOPU6	1:1.6

Characterization. Characterization of modified oils were carried out by gel permeation chromatography (GPC: C-R4A Chrotopac; Shimadzu, Kyoto, Japan). Oils were dissolved in THF by taking 0.1 g/10 mL, and experiments were carried out at a flow rate of 1.0 mL/min using THF as the mobile phase. Columns were calibrated with Aldrich polystyrene standards cross-linked with divinyl benzene. The structures of oils and hybrid materials were characterized by Fourier-transform infrared spectroscopy (FTIR) using a Thermo Nicolet Nexus 670 spectrometer. The ^{1}H and ^{13}C nuclear magnetic resonance spectroscopy (NMR) spectra were recorded in $CDCl_3$ solution using a Varian-Inova 500 MHz spectrometer. The solid state ^{29}Si CPMAS NMR spectra were recorded on a UNITY-400 (Varian, Switzerland) spectrometer connected with high wattage amplifier. A dynamic mechanical thermal analysis (DMTA) IV instrument (Rheometric Scientific, Piscataway, NJ, U.S.A.) in tensile mode at a frequency of 1 Hz with a heating rate of 3 °C/min and scanning the films from −70 to 150 °C has been used to study the viscoelastic properties of the films. Thermogravimetric analysis (TGA) Q500 (TA Instruments, Inc., New Castle, DE, U.S.A.) with a heating rate of 10 °C/min^{-1} under a N_2 atmosphere has been

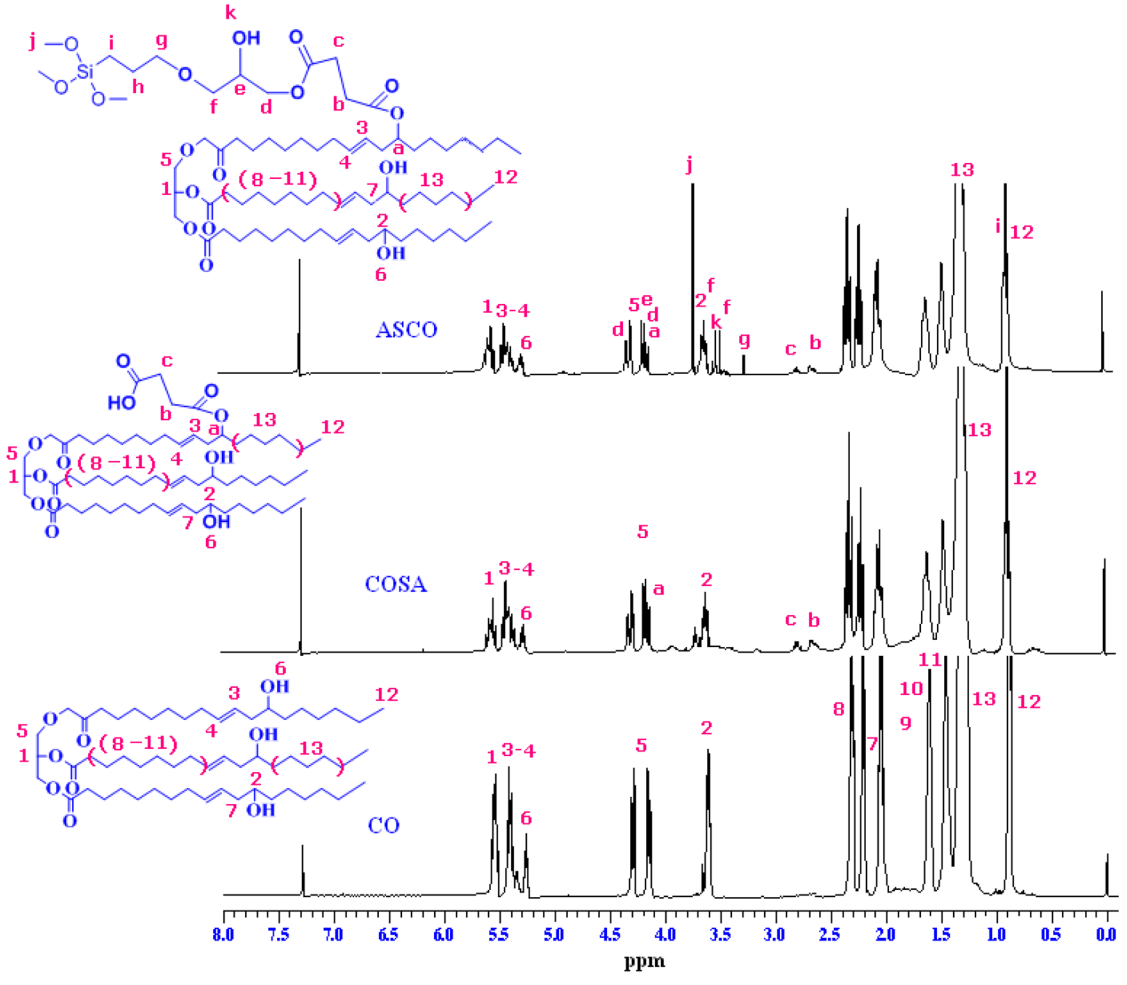

Figure 1. ^{1}H NMR spectrum of CO, COSA, and ASCO.

dx.doi.org/10.1021/sc3001756 | ACS Sustainable Chem. Eng. 2013, 1, 910−918

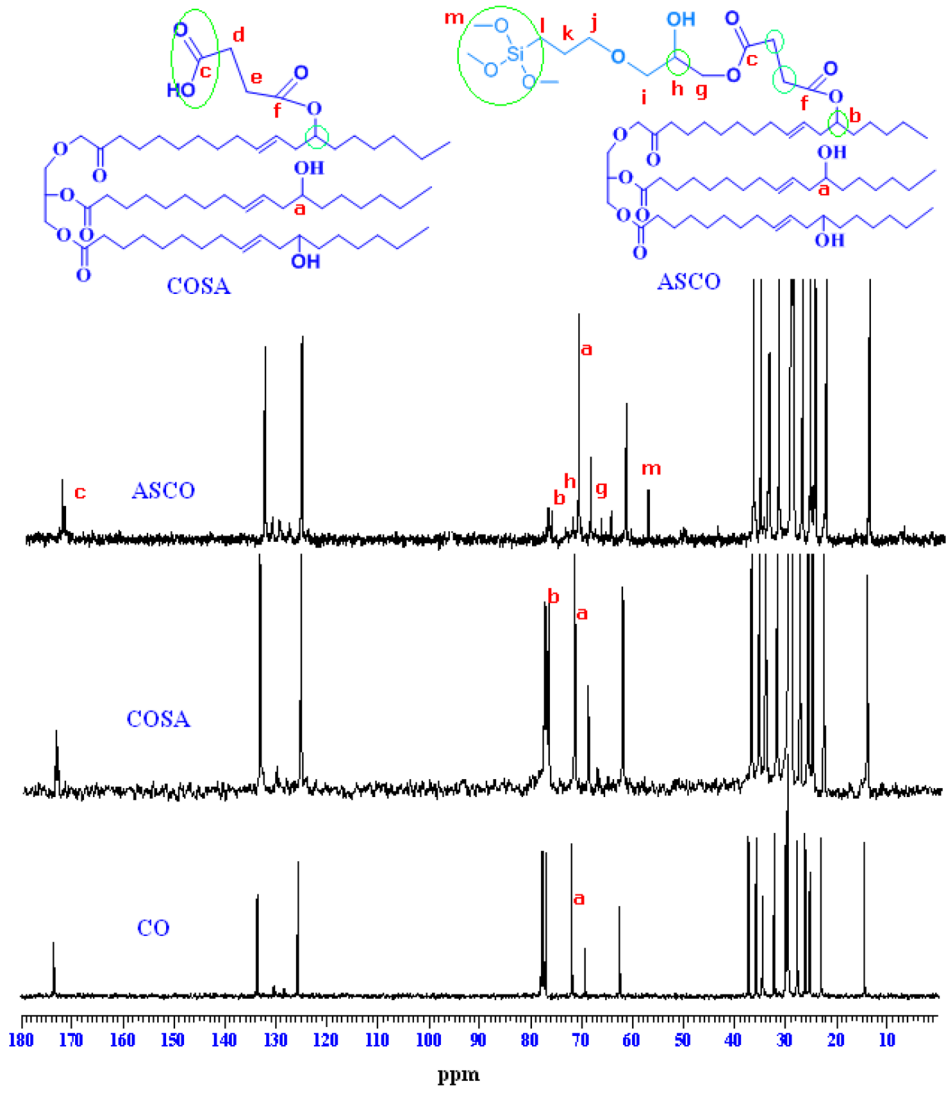

Figure 2. ^{13}C NMR spectrum of CO, COSA, and ASCO.

carried out to study the thermal properties. The differential scanning calorimetry (DSC) analysis was recorded on a Mettler Toledo DSC 821 (Columbus, OH, U.S.A.). The samples were heated from −70 to 150 °C at a heating rate of 20 °C/min under nitrogen atmosphere at a flow rate of 30 mL/min. The viscosity was determined by using a HAAKE rotational viscometer 2.1 system M5/SV2 (Haake, Germany). Contact angle was measured by a G10 (KRUSS) instrument through sessile drop method. Stress−strain measurements were performed on dumbbell-shaped samples cut from the cured free films using Universal Testing Machine (UTM) AGS-10k NG (Shimadzu, Japan). Morphology of the hybrid samples was studied using a Hitachi S520 scanning electron microscope (SEM) instrument operating at 10 kV.

Swelling Properties. The water resistance of the films was measured by calculating the percentage swelling by weight. To do this, preweighed dry films were immersed in deionized water for 50 h to study the water resistance at room temperature. After removing the samples from the immersion bath, they were blotted with soft tissue paper and weighed to calculate the swelling ratio (Q, %) using the following equation.

$$\text{Swelling ratio } (Q)\ \% = [(Ws - Wd)/Wd \times 100]$$

where Wd is the weight of the dry sample and Ws is the weight of the swollen sample.

Toluene Swollen. A known weight (W_0) of cured hybrid films was immersed in a toluene bath for 48 h. The towel-dried sample weight (W_1) and the oven-dried sample weight (W_2) was obtained. Toluene swollen (Wt, %; amount of toluene absorption by hybrid film) and the weight loss (W_L, %; amount of hybrid films dissolved into the toluene solution) of hybrid films in toluene were calculated according to the following equations.

$$Wt\ (\%) = [(W_1 - W_2)/W_2] \times 100$$

$$W_L\ (\%) = [(W_0 - W_2)/W_0] \times 100$$

The volume swelling ratio (qv) of hybrid films was calculated by using following equation.

$$(qv) = Vsw/Vdr$$

where Vsw and Vdr are the volume of the swollen and dried sample, respectively

RESULTS AND DISCUSSION

Characterization of CO, COSA, and ASCO. ^{1}H and ^{13}C NMR spectra of CO, COSA, and ASCO are shown in Figure 1 and 2, respectively. The exact resonance positions have been reported from the expanded spectrum for each resonance area .The ^{1}H NMR spectrum of ASCO was recorded, and the signals are not observed at δ = 3.86 ppm, δ = 2.82 ppm, and δ = 2.68 ppm

dx.doi.org/10.1021/sc3001756 | ACS Sustainable Chem. Eng. 2013, 1, 910−918

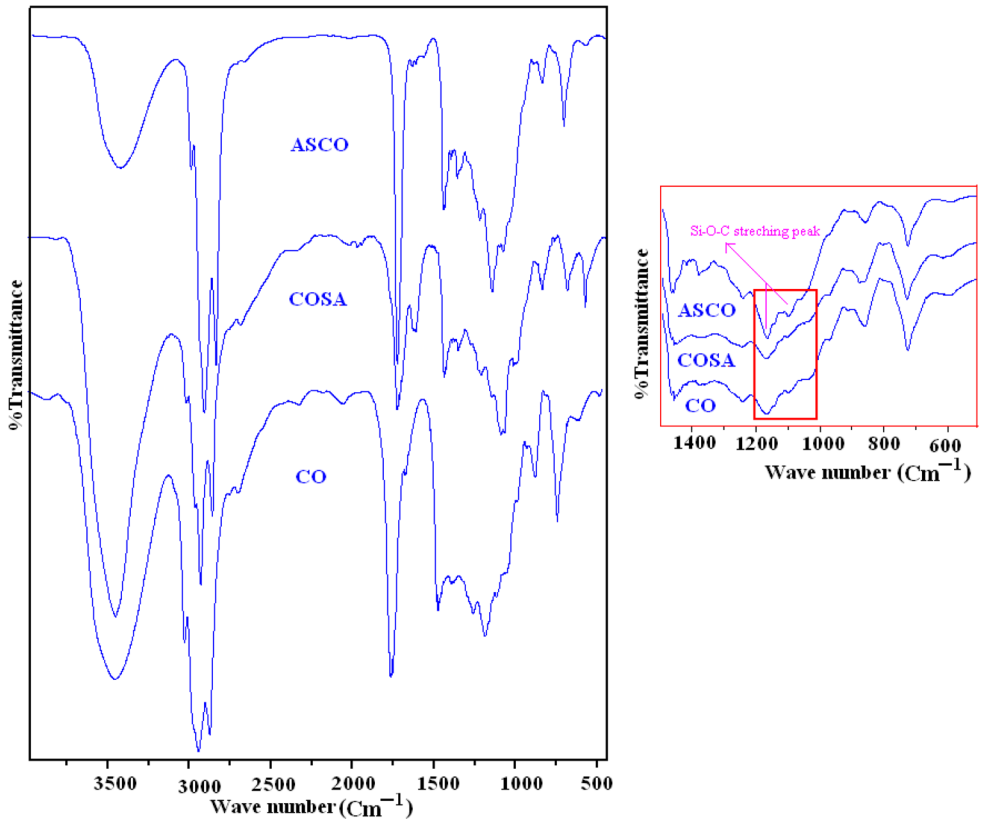

Figure 3. FTIR spectrum of CO, COSA, and ASCO.

due to the methylene group and the two diastereotopic protons of the glycidyl ether groups —OCH_2 (glycidyl), —OCH_2 (epoxy ring), and —OCH_2 (epoxy ring).[21,22] The chemical shifts appearing at 3.56 ppm are associated with methyl protons of Si—OCH_3, indicating methoxysilyl moieties of GPTMS. The spectra of the ASCO show the disappearance of the resonances associated with the methylene group of the epoxy fragment peaks at 45 and 52 ppm because the epoxy ring carbons have not been observed. The signals of the Si $(O\underline{C}H_3)_3$ fragments at 50.5 ppm appear in the final product, and we also found that no signals attributable to the 51−55 ppm region were detected, indicating that the $RSi(OCH_3)_3$ is not involved in hydrolysis and the epoxide ring is not involved in secondary reactions such as homopolymerization or hydrolytic cleavage.[23,24] The spectrum of acid-terminated castor oil is shown in Figure 3. The spectrum shows a significant decrease in hydroxyl groups in the region of 3200−3600 cm^{-1}. This result indicates the reaction of the acid group of COSA with the epoxy group of GPTMS. The progress of the reaction between GPTMS and COSA is studied by FTIR spectroscopy, and the resulting spectrum is shown in Figure 3. In fact, the absorptions due to residual silanol groups and the uncleaved epoxide ring cannot be confidently assigned due to several medium and weak intensity bands in the range of 900−980 cm^{-1}. In our work, the progress of the reaction through the opening of the epoxy rings can be monitored following the decrease in the IR absorption bands associated to −C−H stretching (−C−H stretch in the epoxide) at 3050−2995 cm^{-1} and the disappearance of bands of epoxide at 1260−1240 cm^{-1} (ring breathing). The intensity bands in the range of 1490−1390 cm^{-1} correspond to the bending vibrations of the −C−H bonds. A strong peak near 1090 cm^{-1} is commonly present in the IR spectrum of compounds with a Si−O−C unit, whereas an 1190 cm^{-1} band is typical for Si−O−CH_3 compounds.[25,26] The presence of the −OH group can be seen in the region; it is a broad absorption band peaking around 3500 cm^{-1}. The FTIR spectra of the hybrid films showed (Figure 4) characteristic bands of urethane stretching −N−H at 3500 cm^{-1}, a combination of urethane carbonyl −NH−CO−O and esteric carbonyl −CO−O at 1742 cm^{-1}, and a combination of −N−H

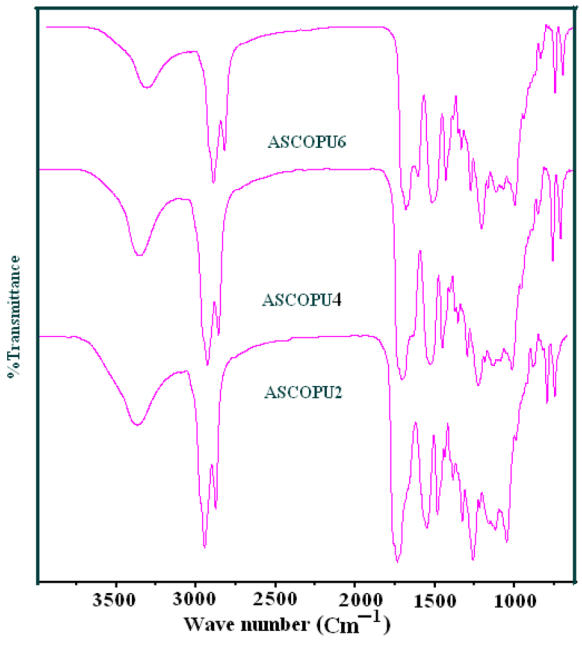

Figure 4. FTIR spectra of cured films.

dx.doi.org/10.1021/sc3001756 | ACS Sustainable Chem. Eng. 2013, 1, 910−918

out-of-plane bending and −C−N stretching at 1532 cm^{-1}. The disappearance of absorption bands at 3400 and 1412 cm^{-1} confirm the absence of free hydroxyl groups in the hybrid. It was also determined that all the castor oil hydroxyl groups had reacted with the −NCO groups of the diisocyanate because the broad band that corresponded to the −OH groups at 3400 cm^{-1} was not detected in the urethane spectra. The intensity of the −N−H vibration region around at 3300 cm^{-1} is higher for hybrid sample with higher a NCO:OH ratio in formulation ASCOPU6. This suggests more urethane linkages. Consequently, more hydrogen bonds may have been formed, and this improves the mechanical properties of the cross-linked polyurethane hybrids. All of the absorbance present in the spectra of the hybrid films are characteristic of castor oil-based hybrid films, symmetric and asymmetric stretching vibration of the aliphatic $-CH_2$ group absorptions at 2,927 and 2856 cm^{-1} for the ester carbonyl functional groups of the triglycerides at1746 cm^{-1}, bending vibrations of the $-CH_2$ and $-CH_3$ aliphatic groups at 1465 cm^{-1}, and $-CH_2$ bending vibrations at 1377 cm^{-1}. FTIR spectra of cured hybrid films show the peak in 1000−1200 cm^{-1} regions is wider for moisture-cured hybrid films in comparison to ASCOPU2; this wider peak is assigned to the overlapping of the peaks corresponding to −Si−O−Si−, −C−Si−O−, and −Si−O−C− stretching. Small bands at 1028.1−1022.2 cm^{-1} relate to the stretching vibrations of −Si−O−Si− from silicates seen only in cured hybrid film and also additional bands at 484 cm^{-1} (−Si−O−Si− bending), 795 cm^{-1}(−Si−O−Si− symmetrical stretching), and 1088 cm^{-1} (−Si−O−Si− asymmetrical stretching) due to the presence of the −Si−O−Si− bond. In addition, the appearance of the peak corresponding to −Si−O stretching vibrations after moisture curing shows that the cross linking was achieved in the moisture-curing process. The broad band between 3000 and 3650 cm^{-1} is due to the Si−OH groups and moisture. The band between 2800 and 3000 cm^{-1} is due to the −CH stretching vibrations (asymmetric $-CH_3$ stretching, 2957 cm^{-1}; asymmetric $-CH_2$ stretching, 2920 cm^{-1}; symmetric $-CH_3$ stretching, 2872 cm^{-1}; and symmetric $-CH_2$ stretching, 2851 cm^{-1}.

Moreover, ^{29}Si NMR studies were carried out to determine the structure of the silica groups in the final polyurethane/urea hybrid films after drying at room temperature for a minimum of 40 days. In Figure 5, the ^{29}Si solid-state NMR spectra of three hybrid films are represented. In the solid-state ^{29}Si NMR spectra, the chemical shift of unsubstituted, mono-, di-, and tri-substituted siloxanes appear at −41, −49, −59, and −68 ppm, respectively.[27] Because GPTMS monomers have trialkoxy silane functionality at each end group, it should form 100% T^3 species when completely condensed. As shown in Figure 5, the peak centered at −68 ppm corresponds to T^3 structure, in which all three hydroxyl groups took part in the condensation reaction. There is no evidence of any peak associated to T^1 or T^0 structures, indicating that the condensation reactions have been almost completed.

The molecular weight and molecular weight distribution of oil-based polymers were monitored by GPC technique. The average molecular weight, polydispersity, and viscosity data of oils are reported in Table 1. It is found that the average molecular weight of ASCO is slightly higher (M_w 1512) in comparison to the molecular weight of COSA and CO (M_w 1442 and 1181, respectively). The viscosities of oils were determined with a rotational viscometer at a shear rate of 23.3 s^{-1}. The viscosities of the modified oils changed in the following order: COSA < ASCO

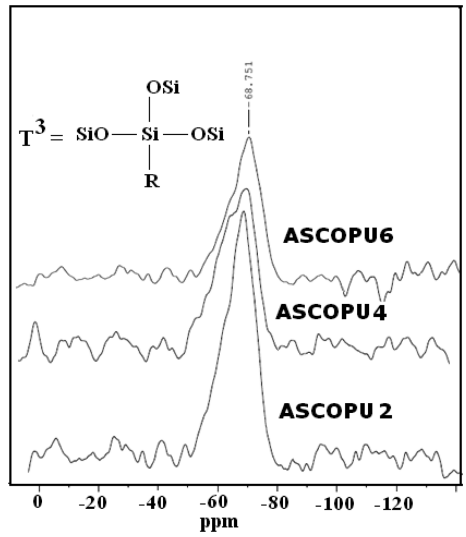

Figure 5. Solid-state ^{29}Si NMR spectrum for hybrid films.

<CO. COSA has the higher viscosity (225 mPa s) in comparison to that of ASCO and CO (225 and 220 mPa s).

The viscoelastic behavior of the hybrid coatings were studied by DMTA instruments, and the results are shown in Figure 6.

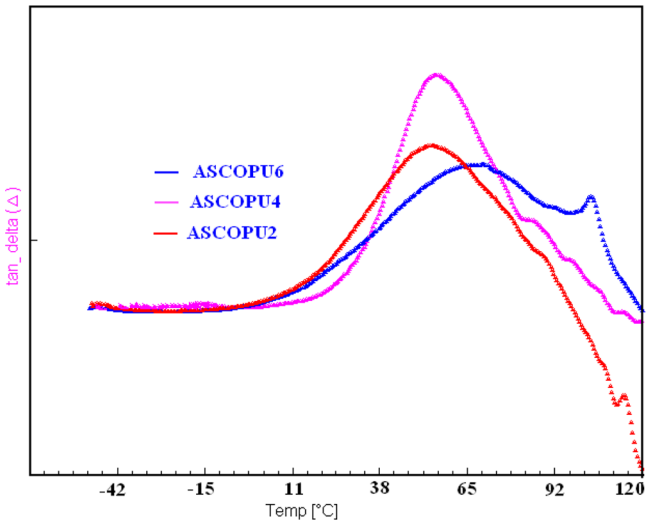

Figure 6. DMTA spectra of hybrid films.

DMTA measures the deformation of a material in response to oscillating forces. The DMTA technique is used to detect the viscoelastic behavior of polymeric materials and yields quantitative results for the tensile storage modulus E′ and the corresponding loss modulus E″. The loss factor tan δ can then be expressed as the quotient of loss and storage, E″/E′. E′ and E″ characterize the elastic and viscous component of a material under deformation, and E′ is a measure of the mechanical energy stored under load. The tan δ compares the amounts of dissipated and stored energy. The *Tg* values of hybrid films are obtained from the peaks of tan δ curves.The cross-link density (υc) of hybrid coatings was calculated by using eq 1.

$$\upsilon c = E'/3RT \quad (1)$$

where *R* is the universal gas constant, and *T* the temperature in K. E′ values in the rubbery region at $T > Tg$ were taken to calculate υe by using eq 1

dx.doi.org/10.1021/sc3001756 | ACS Sustainable Chem. Eng. 2013, 1, 910−918

Table 3. DMTA Data of Hybrid Coatings

sample code	Tg (°C) (DSC)	Tg (°C)	E′ at 30 °C (Pa)	E′ at Tg + 5 °C (Pa)	υc (Tg + 5 °C)(mol/cm^3)
ASCOPU2	18.21	29	2.179×10^7	1.074×10^7	1.402×10^{-3}
ASCOPU4	43.25	57.88	2.745×10^8	1.191×10^7	1.421×10^{-3}
ASCOPU6	56.4	69.77	5.173×10^8	1.326×10^7	1.528×10^{-3}

To observe the effect of the NCO:OH ratio on dynamic mechanical properties, the E ′ and tan δ temperature curves for the representative coating films are shown in Figure 6, while the data is reported in Table 3. The glass transition temperature (Tg), E′ at 30 °C, and cross-link density [calculated at (Tg + 5 °C)] for the samples ASCOPU2, ASCOPU4, and ASCOPU6 are 29, 57.88, and 69.77 °C; 2.179×10^7, 2.745×10^7, and 5.173×10^7 Pa, and 1.402×10^{-3}, 1.421×10^{-3}, and 1.528×10^{-3} mol/cm^3, respectively. These data suggest that the material stiffness, Tg, and cross-linked density of the ASCOPU coatings increases with the increase in the NCO/OH ratio. This figure as well as the data given in Table 3 suggests that the Tg and cross-link density for the above samples increase with increasing NCO content. This may be due to the formation of more urethane/urea segments in the matrix with an increasing NCO/OH ratio, which restricts the chain mobility through hydrogen bonding.[28,29] As shown in Figure 6 and reported in Table 3, the effect of the alkoxy silane group on castor oil has resulted in higher cross-link density, Tg, and E′ as compared to castor oil-based polyurethanes .This may be due to the formed Si−O−Si network and cross-linked structures, which retard segmental motion of the polymer.[30,31]

The effects of the alkoxy silane and NCO content on the tensile strength and percent elongation of the hybrid films are summarized in Table 4. The mechanical behavior of the cross-linked polyurethane hybrids is dependent on the backbone structure of the CO and the NCO:OH ratio, caused by changing the hard segment content, cross-linking density, and intermolecular interactions between their hard segments. This happens due to the presence of close packing in the polymer matrix because of the Si−O−Si network of the ASCO, which in turn does not allow the polymer to stretch for long and thus increases the tensile strength and decreases the elongation.

Table 4. Tensile Properties Data of Hybrid Films

sample code	tensile strength (N/mm^2)	max. displacement (mm)	% elongation
ASCOPU2	4.2	47.16	100.04
ASCOPU6	11.3	28.33	78.15
ASCOPU8	14.1	25.22	56.98

TGA is used to measure a variety of polymeric phenomenon involving weight changes, sorption of gases, desorption of contaminant, and degradation. The thermal degradation study of CO, COSA, and ASCO were done in a N_2 environment at a heating rate of 10 °C/min. Figure 7 shows the TGA and derivative mass loss (DTG) thermograms for CO, COSA, and ASCO; two-step decomposition profiles were observed. It was noticed from the TGA profile that the thermal stability of ASCO is higher than that of both CO and COSA, respectively. The main decomposition of the samples takes place in the second stage of degradation, i.e., above the temperature 368 °C. The values of T_{on} (initial decomposition temperature for degradation step), T_{end} (final decomposition temperature for degradation step), and % weight remaining at 350, 450, and 550 °C are summarized in Table 5. These values clearly suggest that thermal stability is high for ASCO. The increase in thermal stability might be attributed due to the hydrogen bridges between −OH groups, ester carbonyl OH groups, and the −Si−OCH$_3$ group. The TGA curves of hybrid coatings are shown in Figure 8. All the hybrid samples show a three-step degradation profile. The data shows that the thermal stability of the hybrid samples is increased with increasing the NCO:OH ratio. For instance, the onset degradation temperature and wt % remaining at 550 °C for the samples ASCOPU2, ASCOPU4, and ASCOPU6 are 306.2, 309.3, and 313.9 °C and 1.3, 1.7, and 2.5 wt %, respectively. This

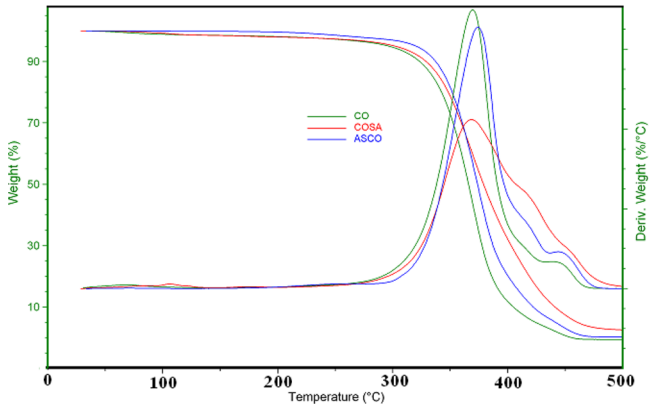

Figure 7. TGA and DTG curves of CO, COSA, and ASCO.

Table 5. Thermal Analysis Data of Hybrid Coatings

			% weight remaining		
sample name	T_{on}	T_{end}	350 °C	450 °C	550 °C
CO	374.3	435.8	83.2	3.12	0.27
COSA	369.2	445.2	72.63	0.69	0.01
ASCO	372.8	461.3	78.25	7.41	2.23
ASCOPU2	306.2	452.5	42.8	4.52	1.3
ASCOPU4	309.3	459.3	43.75	4.85	1.7
ASCOPU6	313.9	466.6	46.5	5.46	2.15

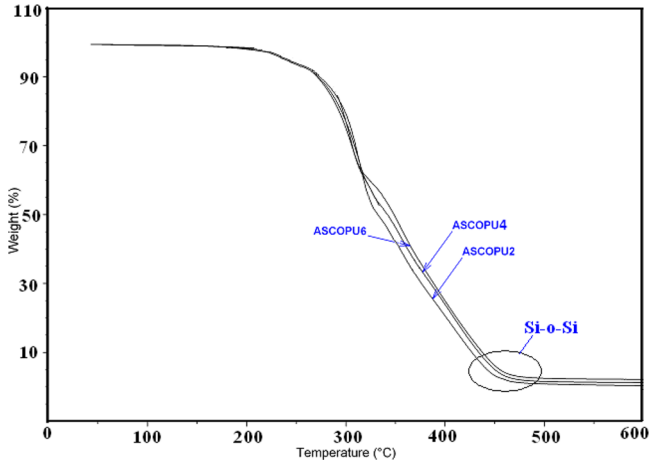

Figure 8. TGA curves of different hybrid films.

dx.doi.org/10.1021/sc3001756 | ACS Sustainable Chem. Eng. 2013, 1, 910−918

trend indicates formation of more cross-linked and hydrogen-bonded structures at a higher NCO/OH ratio. More cross-linking, the formed Si−O−Si linkages, and hydrogen bonding brings the polymer backbones closer and thus reduces the molecular mobility and increases the thermal stability. This behavior also supports the increase in *T*g of the samples with an increase in the NCO/OH ratio in the DMTA analysis.[32−34] The analysis indicates the alkoxy silane content in the samples has resulted in the corresponding increase in T_{on}, 50% wt % loss temperature, and char residue. ASCOPU6 hybrid films from ASCO act as thermal insulators and mass transfer barriers (by acting as a well packing material) for the volatile organic compounds generated during heating, thus increasing the thermal stability and final char residue of the hybrid coatings. The glass transition temperature (*T*g) properties of the films were studied by DSC; their results are displayed in Figure 9 and

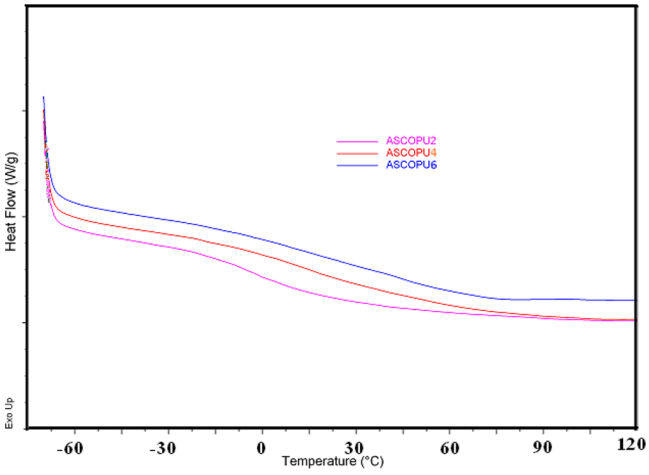

Figure 9. DSC curves of different hybrid films.

reported in Table 3. The glass transition temperature of ASCOPU2, ASCOPU4, and ASCOPU6 coatings are 18.21, 43.25, and 56.4 °C, respectively. The DMTA technique generally provide higher *T*g values than DSC due to the dynamic nature of test.[35]The glass transition temperature increases with increasing NCO:OH ratio, so it seems reasonable to assume that the mobility of organic polyurethane chains is greatly restricted by a hard inorganic Si−O−Si network. The effect might be observed due to the high cross-linking density of the hybrid by increasing the cross linker, which restricted the segmental motion of the polymer chains and increased the glass transition temperature. The water contact angle was in the range of 75°−82°. The contact angle data of the hybrid films are reported in Table 6. It can be confirmed that the improvement of the hydrophobic capacity of hybrid films occurred by increasing the NCO:OH ratio due to the formation of Si−O−Si linkage by the moisture curing process. Table 6 shows the water and toluene swelling as a function of immersing time of the hybrid-cured films. The swelling ratio measurements of the cured films can be used to observe water resistance and hydrophobicity. This suggests that there exists sufficiently high cross-link density in these films, which enables the swelling behavior to outweigh the weight loss caused by water-soluble oil segments or only slightly cross-linked ones. All of the films exhibited significant swelling in toluene and chloroform; this varied with NCO:OH ratio, as shown in Table 6.

The typical morphologies of hybrid films shows that there is no phase separation in pure polyurethane and discrete phase observed in all the hybrid composite films, indicating that the siloxane phase shows homogeneous distribution and good interfacial interaction. Figure 10a, b, and c indicate that a good interaction between organic and inorganic phases could be due to the formation of Si−O−C bond

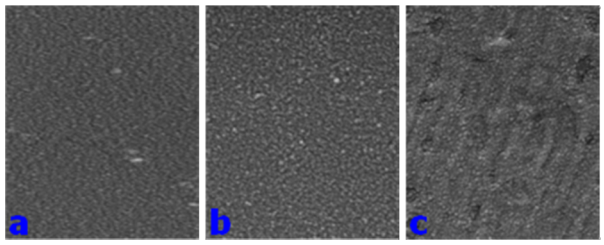

Figure 10. SEM micrographs of hybrid films: (a) ASCOPU2, (b) ASCOPU4, and (c) ASCOPU6.

CONCLUSIONS

An attempt has been made to develop renewable resource-based polyurethane silica hybrid coatings using castor oil. For this purpose, a novel methodology has been used for the synthesis of alkoxy silane functional castor oil that was further reacted with different ratios of isophorone diisocyanate to get an isocyanate-terminated silica hybrid polyurethane prepolymer. The excess isocyanate of the prepolymers was cured under atmospheric moisture to get polyurethane/urea−silica hybrid coatings. A detailed spectroscopic investigation has been carried out to confirm the structures of alkoxy silane castor oil, prepolymers, and coatings. Coatings were studied for thermal, tensile, and viscoelastic properties using different techniques. The coating properties such as swelling and contact angle were also measured. The swelling properties and contact angle were directly dependent on the NCO:OH ratio. The hydrophobic character of the hybrid coating films were found to increase with an increasing NCO/OH ratio. The alkoxy silane-modified castor oil-based coatings shows better mechanical and viscoelastic properties in comparison to the control (unmodified CO) coatings. The oil chains are chemically connected to the silica functional group, and the incorporation of silica not only works as a reinforcement filler but also increases the cross-link density and thermal properties of the castor oil, which is evidenced by the higher thermo-mechanical properties measured by DMTA and

Table 6. Swelling and Contact Angle Data of the Hybrid Films[a]

sample code	contact angle (θ)	W_{st} (%)	W_{dt} (%)	*q*vt	W_{sc} (%)	W_{dc} (%)	*q*vc	Q (%)
ASCOPU2	74	114.61	15.59	2.14	181.26	18.91	2.81	0.85
ASCOPU4	76	86.75	8.92	1.86	129.73	12.47	2.29	0.46
ASCOPU6	82	76.85	6.96	1.76	102.28	9.51	2.02	0.35

[a]W_{st}: toulene absorption by hybrid film.W_{dt}: hybrid film dissolved in toulene. *q*vt: volume swelling ratio hybrid film in toluene. W_{sc}: chlroform absorption by hybrid film.W_{dc}: hybrid film dissolved in chlroform. *q*vc: volume swelling ratio hybrid film in chloroform.

dx.doi.org/10.1021/sc3001756 | ACS Sustainable Chem. Eng. 2013, 1, 910−918

UTM. The synthetic method developed for hybrid films indicates that a novel strategy can become hybrid without the use of organo-silane functional compounds. Hence, this work provides an effective and promising way to prepare hydrolyzable silane plant oils for high performance hybrid coatings.

AUTHOR INFORMATION

Corresponding Author

*E-mail: kvsnraju@iict.res.in. Telefax: +91-40-27193991.

Notes

The authors declare no competing financial interest.

ACKNOWLEDGMENTS

Shaik Allauddin thanks the Council of Scientific and Industrial Research (CSIR), New Delhi, India, for a research fellowship.

REFERENCES

(1) Hiroshi, U.; Mai, K.; Takashi, T.; Mitsuru, N.; Arimitsu, U.; Shiro, K. Green nanocomposites from renewable resources: Plant oil−clay hybrid materials. *Chem. Mater.* **2003**, *15*, 2492−2494.

(2) Ogunniyi, D. S. Review paper castor oil: A vital industrial raw material. *Bioresour. Technol.* **2006**, *97*, 1086−1091.

(3) Petrovic, Z. S. Polyurethanes from vegetable oils. *Polym. Rev.* **2008**, *48*, 109−155.

(4) Xie, H. Q.; Guo, J. S. Room temperature synthesis and mechanical properties of two kinds of elastomeric interpenetrating polymer networks based on castor oil. *Eur. Polym. J.* **2002**, *38*, 2271−2277.

(5) Black, M.; Rawlins, J. W. Thiol-ene UV-curable coatings using vegetable oil macromonomers. *Eur. Polym. J.* **2009**, *45*, 1433−1441.

(6) Cakic, S. M.; Ristic, I. S.; Djordjevic, D. M.; Stamenkovic, J. V.; Stojiljkovic, D. T. Effect of the chain extender and selective catalyst on thermooxidative stability of aqueous polyurethane dispersions. *Prog. Org. Coat.* **2010**, *67*, 274−280.

(7) Sanchez, C.; de A, G. J.; SolerIllia, A.; Ribot, F.; Lalot, T.; Mayer, C. R.; Cabuil, V. Designed hybrid organic−inorganic nanocomposites from functional nanobuilding blocks. *Chem. Mater.* **2001**, *13*, 3061−3083.

(8) Witucki, L. G. A silane primer: Chemistry and applications of aikoxy silanes. *J. Coat. Technol.* **1993**, *65*, 57−60.

(9) Kinloch, A. J. *Adhesion and Adhesives: Science and Tecnology*; Chapman and Hall, New York, 1987.

(10) Tsujomoto, T.; Uyama, H.; Kobayashi, S. Green nanocomposites from renewable resources: biodegradable plant oil−silica hybrid coatings. *Macromol. Rapid Commun.* **2003**, *24*, 711−714.

(11) Colak, S.; Kusefoglu, S. H. Synthesis and interfacial properties of aminosilane derivative of acrylated epoxidized soybean oil. *J. Appl. Polym. Sci.* **2007**, *104* (4), 2244−2253.

(12) Lligadas, G.; Callau, L.; Ronda, J. C.; Galia, M.; Cadiz, V. Novel organic−inorganic hybrid materials from renewable resources: Hydrosilylation of fatty acid derivatives. *J. Poly. Sci: Part A: Poly. Chem.* **2005**, *43* (24), 6295−6307.

(13) Wold, C. R.; Soucek, M. D. Viscoelastic and thermal properties of linseed oil-based ceramer coatings. *Macromol. Chem. Phys.* **2000**, *201* (3), 382−392.

(14) Deffar, D.; Teng, G.; Soucek, M. D. Comparison of titanium-oxo-clusters derived from sol-gel precursors with TiO_2 nanoparticles in drying oil based ceramer coatings. *Macromol. Mater. Eng.* **2001**, *286*, 204−215.

(15) Jiménez, R.; Téllez, L.; Rodríguez, L. M.; San, J. Modulation of the hydrophilic character and influence on the biocompatibility of polyurethane−siloxane based hybrids. *Bol. Soc. Esp. Ceram. Vidrio* **2011**, *50*, 1−8.

(16) Lligadas, G.; Ronda, J. C.; Galià, M.; Cádiz, V. Novel silicon-containing polyurethanes from vegetable oils as renewable resources. Synthesis and properties. *Biomacromolecules* **2006**, *7*, 2420−2426.

(17) Lligadas, G.; Ronda, J. C.; Marina, G.; Cadiz, V. Bionanocomposites from renewable resources: Epoxidized linseed oil−polyhedral oligomeric silsesquioxanes (POSS) hybrid materials. *Biomacromolecules* **2006**, *7*, 3521−3526.

(18) Hiroshi, U.; Mai, K.; Takashi, T.; Mitsuru, N.; Arimitsu, U.; Shiro, K. Green nanocomposites from renewable resources: Plant oil−clay hybrid materials. *Chem. Mater.* **2003**, *15*, 2492−2494.

(19) Maria, A.; de, Luca.; Márcia, M.; Cláudia, C.T. B. Hybrid films synthesised from epoxidised castor oil, glycidoxy propyl trimethoxysilane and tetraethoxysilane. *Pro. Org. Coat.* **2009**, *65*, 375−380.

(20) Hiroshi, U.; Mai, K.; Takashi, T.; Mitsuru, N.; Arimitsu, U.; Shiro, K. Organic−inorganic hybrids from renewable plant oils and clay. *Macromol. Biosci.* **2004**, *4*, 354−360.

(21) Innocenzi, P.; Sassi, A.; Brusatin, G.; Guglielmi, M.; Favretto, D.; Bertani, R.; Venzo, A.; Babonneau, F. A novel synthesis of sol-gel hybrid materials by a nonhydrolytic/hydrolytic reaction of (3-glycidoxypropyl) trimethoxysilane with $TiCl_4$. *Chem. Mater.* **2001**, *13* (10), 3635−3643.

(22) Torry, S. A.; Campbell, A.; Cunliffe, A. V.; Tod, D. A. Kinetic analysis of organosilane hydrolysis and condensation. *Int. J. Adhes. Adhes.* **2006**, *26*, 40−49.

(23) Templin, M.; Wiesner, U.; Spiess, H. A. Multinuclear solid-state-NMR studies of hybrid organic−inorganic materials. *Adv. Mater.* **1997**, *9* (10), 814−817.

(24) Cardiano, P.; Sergi, S.; Lazzari, M.; Piraino, P. Epoxy−silica polymers as restoration materials. *Polymer* **2002**, *43* (5), 6635−6640.

(25) Nishiyama, N.; Horie, K.; Asakura, T. Adsorption behavior of a silane coupling agent onto a colloidal silica surface studied by ^{29}Si NMR spectroscopy. *J. Colloid Interface Sci.* **1989**, *129*, 113−119.

(26) Jack, K.; Crandall, C. M. Siloxanes from the hydrolysis of isopropyltrimethoxysilane. *J. Organomet. Chem.* **1995**, *489*, 5−13.

(27) Kahraman, M. V.; Kugu, M.; Menceloglu, Y.; Nilhan, K. A.; Atilla, G. The novel use of organo alkoxy silane for the synthesis of organic−inorganic hybrid coatings. *J. Non-Cryst. Solids* **2006**, *352*, 2143−2151.

(28) Fu, J. F.; Shi, L. Y.; Yuan, S.; Zhong, Q. D.; Zhang, D. S.; Chen, Y.; Wu, J. Morphology, toughness mechanism, and thermal properties of hyperbranched epoxy modified diglycidyl ether of bisphenol A (DGEBA) interpenetrating polymer networks. *Polym. Adv. Technol.* **2008**, *19* (11), 1597−1607.

(29) Jena, K. K.; Raju, K. V. S. N. Synthesis and characterization of hyperbranched polyurethane−urea/silica based hybrid coatings. *Ind. Eng. Chem. Res.* **2007**, *46* (20), 6408−6416.

(30) Gireesh, K. B.; Kishore, K. J.; Allauddin, S.; Radhika, K. R.; Ramanuj, N.; Raju, K. V. S. N. Structure and thermo-mechanical properties study of polyurethane−urea/glycidoxypropyltrimet hoxysilane hybrid coatings. *Pro. Org. Coat.* **2010**, *68*, 165−172.

(31) Pion, F.; Jena, K. K.; Allauddin, S.; Ramanuj, N.; Raju, K. V. S. N. Preparation and characterization of waterborne hyperbranched polyurethane−urea and their hybrid coatings. *Ind. Eng. Chem. Res.* **2010**, *49* (10), 4517−4527.

(32) Dutta, S.; Karak, N. Effect of the NCO/OH ratio on the properties of *Mesua ferrea* L. seed oil-modified polyurethane resins. *Polym. Int.* **2006**, *55*, 49−56.

(33) Asif, A.; Shi, W. UV curable waterborne polyurethane acrylate dispersions based on hyperbranched aliphatic polyester: Effect of molecular structure on physical and thermal properties. *Polym. Adv. Technol.* **2004**, *15* (11), 669−675.

(34) Mishra, A. K.; Allauddin, S.; Radhika, K. R.; Narayan, R.; Raju, K. V. S. N. Effect of NCO/OH ratio and Ce−Zr nanoparticles on the thermo-mechanical properties of hyperbranched polyurethane urea coatings. *Polym. Adv. Technol.* **2011**, *22*, 882−890.

(35) Darren, J. M.; Gordon, F. M.; Gordon, M. R.; Pathiraja, A. G.; Simon, J. M. Effect of soft-segment CH_2/O ratio on morphology and properties of a series of polyurethane elastomers. *J. Appl. Polym. Sci.* **1996**, *60* (4), 557−571.